Agroforest Syst (2026) 100:211
https://doi.org/10.1007/s10457-026-01573-w

Effects of tree-stripes on crop growth in agroforestry systems using unmanned aerial systems-based analysis

Timo Kunzmann · Carsten Neumann · Nicole Koellner

Received: 23 March 2025 / Accepted: 9 June 2026

Abstract Agroforestry systems (AFS) offer a promising strategy to address environmental challenges while supporting rising food demands. However, the complex interactions between trees and crops complicate research, particularly regarding their effects on crop yields. This study presents a methodological approach using multispectral unmanned aerial system (UAS) data to investigate a maize-cultivated alley cropping system in eastern Germany as a case study. Growth parameters, namely the Normalized Difference Vegetation Index (NDVI) and plant height, were derived as proxies for yield and analyzed in relation to the distance from tree stripes. Additionally, direction-dependent regression analyses were conducted to assess whether spatial variations in the field could be attributed to the trees. Two distinct patterns emerged: first, a pronounced increase in NDVI was observed at close proximity to the trees, correlated with tree height and schematically illustrated for two representative tree stripes; second, at greater distances, fluctuations in NDVI were associated with the trees but lacked consistent directional trends. Considerable inconsistencies were also observed in plant height variations. The discussion highlights potential drivers of the close-range NDVI increase, the applicability of UAS for AFS research, and limitations in generalizing findings from a single case study. Overall, the results demonstrate that tree effects on crop growth and vitality are detectable but marginal in terms of their influence on maize yields at this site, while showcasing the utility of UAS-based approaches for field-scale analysis of AFS.

Keywords Agroforestry systems · UAS · Crop yields · Plant heights · Vitality

T. Kunzmann (✉) · C. Neumann · N. Koellner
Section of Remote Sensing and Geoinformatics, GFZ Helmholtz Centre for Geosciences, Telegrafenberg, 14473 Potsdam, Germany
e-mail: kunzmanntimo@gmail.com

T. Kunzmann
Institute of Geography and Geoecology, Karlsruhe Institute of Technology (KIT), Kaiserstr. 12, 76131 Karlsruhe, Germany

Introduction

Agroforestry—a complex agroecological system

Agroforestry is a long-established global land use management system that is currently receiving renewed attention in Europe (Mosquera-Losada et al. 2012; Sollen-Norrlin et al. 2020; Santiago-Freijanes et al. 2021; Thiesmeier & Zander 2023). In modern times, when population growth and increasing food demand conflict with the conservation of environmental resources (Davis et al. 2016; Molotoks et al. 2021), agroforestry can play a key role in reconciling both sides (Smith, Pearce and Wolfe, 2013). It is a promising method to mitigate the effects of climate

Published online: 04 July 2026

change (Dmuchowski, Baczewska-Dąbrowska and Gworek, 2024) while stabilizing agroecosystems through microclimatic effects and improved water balance (Jacobs et al. 2022). In temperate Europe, alley cropping systems (ACS), where trees are grown alongside crops, are less widespread than systems integrating trees with livestock (Mosquera-Losada et al. 2023). Alley Cropping Systems work by planting parallel stripes of trees and hedges in agricultural fields at intervals of 5–100 m, depending on light conditions and the spatial requirements of the intercrops. Beneficial ecological effects have been described, such as windbreak effects (Böhm, Kanzler and Freese, 2014; Weninger et al. 2021; Brandle et al. 2021), which increase water availability (Zhu et al. 2020; Kaushal et al. 2021) and improve water quality (Tsonkova et al. 2012; Awazi et al. 2024). Soils are affected through reduced erosion (Palma et al. 2007; Tsonkova et al. 2012) and nutrient leaching (Quinkenstein et al. 2009; Pardon et al. 2017; Zhu et al. 2020; Sileshi et al. 2020; Kim & Isaac 2022), as well as increased fertility (Beuschel et al. 2019; Sileshi et al. 2020) and carbon sequestration (Shi et al. 2018; Mayer et al. 2022; Ghale et al. 2022). At the landscape level, such systems benefit habitat and species diversity (Quinkenstein et al. 2009; Torralba et al. 2016). However, due to multiple overlapping effects, it remains challenging to quantify individual agroecological contributions, which is necessary to assess their ecological benefits while also understanding impacts on crop productivity.

Remote sensing and UASs for agroforestry

The integration of modern imaging techniques with machine learning offers a powerful approach to map and disentangle ecological processes within agroforestry landscapes, particularly by capturing their spatiotemporal dynamics. Remote sensing enables the acquisition of high-dimensional image data, facilitating spatially explicit and temporally dense analyses. Satellite-based remote sensing has been employed to examine tree impacts on crop yield at the landscape level (Leroux et al. 2020; Yang et al. 2020) and to estimate aboveground vegetation biomass in agroforestry systems (Thapa, Lovell and Wilson, 2023). A contemporary and cost-effective approach is that of UAS-borne remote sensing, which, unlike satellite analyses, allows for the derivation of spatially high-resolution information. Over recent years, UASs have gained increasing attention in agricultural applications (Tsouros, Bibi and Sarigiannidis, 2019), as they allow repeated imaging of field-level variability at relatively low cost. When combined with machine learning, UAS imagery permits the derivation of plant and soil parameters, including plant height, growth rate (Holman et al. 2016), crop yields (Nevavuori, Narra and Lipping, 2019), and water stress indicators (Gago et al. 2015).

A key advantage of UASs is their capacity to provide comprehensive, high-resolution datasets without extensive manual sampling, which is particularly valuable given the complex interactions of factors in agroforestry systems (Golicz et al. 2023). Accurate interpretation of such data requires robust statistical methods and large numbers of sampling plots. Although UAS technology has demonstrated its potential for ecological studies (Pádua et al. 2017), its application specifically in agroforestry research remains limited. Wengert et al. (2021) note that previous research predominantly relies on terrestrial measurements along transects with limited spatial resolution, ranging from 3 to 24 m. They demonstrated the potential of UASs to assess spatial variability in crop yield and leaf area index. Further studies using UASs include Iwasaki et al. (2019), which assessed the impact of trees on the NDVI of maize plants and the subsequent effect on yields; a preliminary investigation into tree effects on NDVI was also conducted by Roupsard et al. (2020) using geostatistical techniques. Lastly, Bolívar-Santamaría and Reu (2024) applied UASs to assess habitat complexity using 3D point clouds.

Building on these studies, the present work aims to demonstrate the methodological applicability of UAS-based remote sensing for analyzing agroforestry systems by extracting plant parameters from high-resolution imagery and translating them into spatially explicit indicators of crop performance. To illustrate this potential, the approach is applied to a temperate European agroforestry system as a case study, providing a methodological framework rather than a broadly generalizable evaluation. The specific research objectives outlined below should be understood within the context of this methodological framework.

Crop yields in temperate European agroforestry

Beyond ecological effects, estimating productivity through crop yields is essential to assess the economic viability of agroforestry systems alongside their environmental benefits. Majaura, Böhm, and Freese (2024) highlight substantial variability in yields arising from factors such as tree or crop species and the structural arrangement of tree–crop configurations. It is therefore important to investigate how tree-stripes influence productivity. In proximity to trees, crop yields are often reduced within a "competition zone" (1–2 × tree height) due to resource competition, shading, allelopathic effects, and microclimatic changes. Conversely, in zones located 3–10 × tree height, yields may increase due to improved microclimatic conditions and enhanced soil moisture (Majaura, Böhm and Freese, 2024). This characteristic pattern is frequently referred to as a bell-shaped yield curve. Understanding these spatial zones and their controlling factors is crucial for the design of agroforestry field layouts.

UAS technology facilitates the examination of spatial growth patterns as proxies for crop yields, enabling quantification of plant vitality relative to tree proximity. Accordingly, the objectives of this study are:

- To ascertain whether UAS imagery can be used to identify spatial patterns of plant growth and plant vitality for segmented individuals of the same species (maize) within an agroforestry system.
- To determine whether observed patterns can be attributed to the planting and height of tree-stripes.
- To ascertain the distance up to which tree-stripes exert an influence on maize growth and vitality as yield indicator.

Methods

Study area

The study was conducted in a short-rotation silvoarable alley cropping system (Nair 1985) in the Lausitz region (51°27′32.328'' N, 13°58′18.4368'' E), south-east Brandenburg, Germany, covering approximately 0.25 km^2. The site has a gentle gradient of 1:250, descending towards the south-west. Soils are classified as Gleyic Cambisol (IUSS Working Group WRB 2022), with medium sandy texture (Geoportal LBGR Brandenburg 2024) and poor water retention (Drastig et al. 2011). Nearby Cottbus has an annual mean temperature of 10.4 °C and precipitation of 685 mm, reflecting low rainfall typical of southern Brandenburg, which contributes to lower crop yields (Drastig et al. 2011). During 2023, a pre-summer drought was followed by average summer rainfall (Deutscher Wetterdienst 2023). Mean annual wind speeds are ~ 25 km/h, primarily from westerly directions (Kasperski 2002; Neil et al., 2023).

Maize was planted across the field in early May 2023. Compared to surrounding fields, the crop showed markedly reduced growth heights. The farmer reported minimal pesticide application and exclusive use of organic fertilizers. Maize was sown in parallel rows spaced 70–80 cm apart, with inter-row spaces occupied by diverse weed species, varying in abundance across the field. Growth was patchy, with areas of uniform height several meters wide (Fig. 2), and soil moisture increased from east to west.

Six wooden tree stripes were planted in a north–south direction (Fig. 1), each comprising three rows of trees or bushes of different species. Planted in 2013, stripes varied in width (10–30 m) and tree height (2–13 m at data acquisition, Fig. 2). Although species composition is important for AFS effects (Majaura, Böhm and Freese, 2024), it was not considered due to lack of data.

UAS data acquisition and processing

Data were collected on September 6, 2023, between 11:00 and 12:30 under clear sky conditions. A DJI Phantom 4 Multispectral drone equipped with five monochrome sensors (Blue: 450 ± 16 nm, Green: 560 ± 16 nm, Red: 650 ± 16 nm, Red-Edge: 730 ± 16 nm, NIR: 840 ± 26 nm) was flown at 60 m altitude, yielding a 3.1 cm ground sampling distance with 75% frontal and side overlap. A white reference panel (Spectralon®, 50%) enabled radiometric calibration, and the upward-facing sun sensor allowed computation of physical reflectance despite varying solar intensity. Post-processing kinematics (PPK) applied to GNSS coordinates achieved sub-cm positional accuracy, automatically georeferencing the

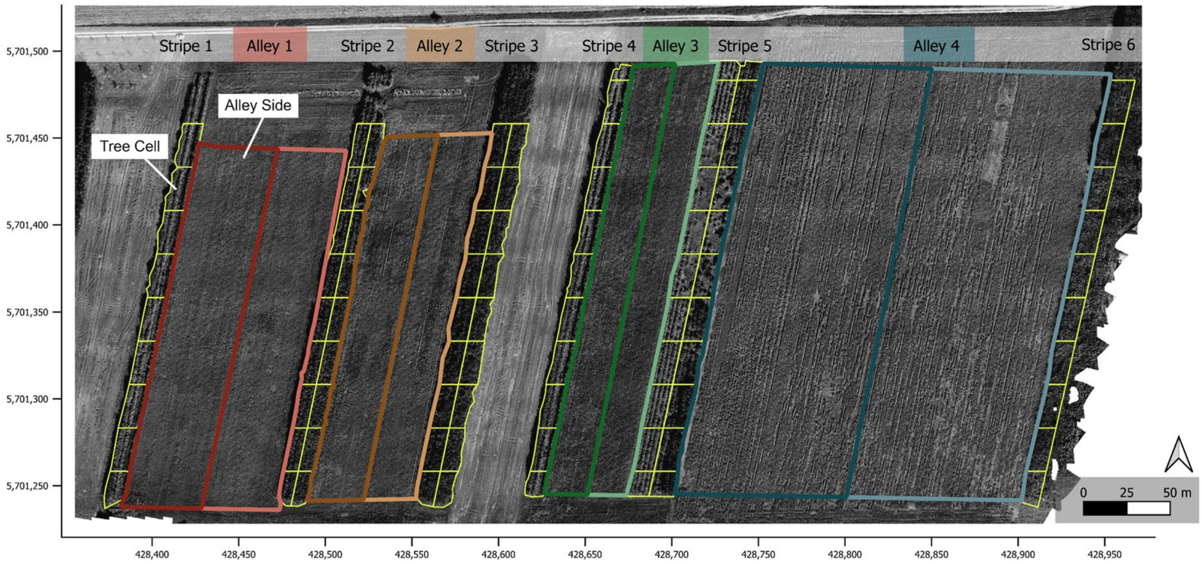

Fig. 1 The UAS orthomosaic depicts the boundaries of individual alleys, delineated as coloured polygons. These alleys are distinguished as either west or east, and the tree stripes are visible running in north–south direction through the field. They are delimited by 25 m long yellow cells in which the average tree height was calculated

orthomosaic without ground control points (Zhang et al. 2019).

To validate plant height derivation, 106 maize plants were measured in the field using a folding ruler, with GPS-recorded coordinates. Only maize from uniform-height patches (see section: Study Area) was sampled to mitigate GPS inaccuracies. Images were processed in Agisoft Metashape (Agisoft LLC, 2023), generating a digital surface model (DSM) and orthomosaic using structure-from-motion.

Maize classification

To extract NDVI and plant heights solely from maize plants, while excluding surrounding soil or weeds, the maize was segmented using a combination of dynamic thresholding and a random forest classifier.

Dynamic thresholding (Niblack, W., 1986) is a method that highlights objects by comparing their albedo to the background of the image. Due to the high growth rate of the maize plants, they were exposed to direct sunlight while simultaneously shading the surrounding lower-growing weeds and soil. This results in albedo discrepancies, which could be used for classification. In order to calculate the albedo, the grey values of all five bands were aggregated for each pixel. The background surrounding a plant was estimated by applying a mean filter to the albedo image (window size: 51×51px). Subsequently, each pixel was compared to the background. Pixels that met the condition *pixel * 0.7 > background* were segmented as maize plants. The parameters were adjusted so that the maize was classified with greater precision. This resulted in a segmented pixel being very likely to belong to a maize plant (low false positives), while not all true maize pixels were identified (high false negatives).

Remaining unclassified areas (bare soil) were processed with a Random Forest classifier (Breiman 2001) using 91 training polygons to separate maize, weeds, and soil. No ground-truth coverage was available; polygons were visually delineated on the orthomosaic. Both classification outputs were combined, keeping only pixels classified as maize by both methods, followed by a 3×3 px majority filter (Kim, 1996) to remove isolated misclassifications (Fig. 2).

Derivation of plant heights

The derivation of plant heights involved creating a normalized digital surface model (nDSM) and determining individual plant positions: First, a substantial number of ground points (n = 125) representing exposed soil were identified within the orthomosaic,

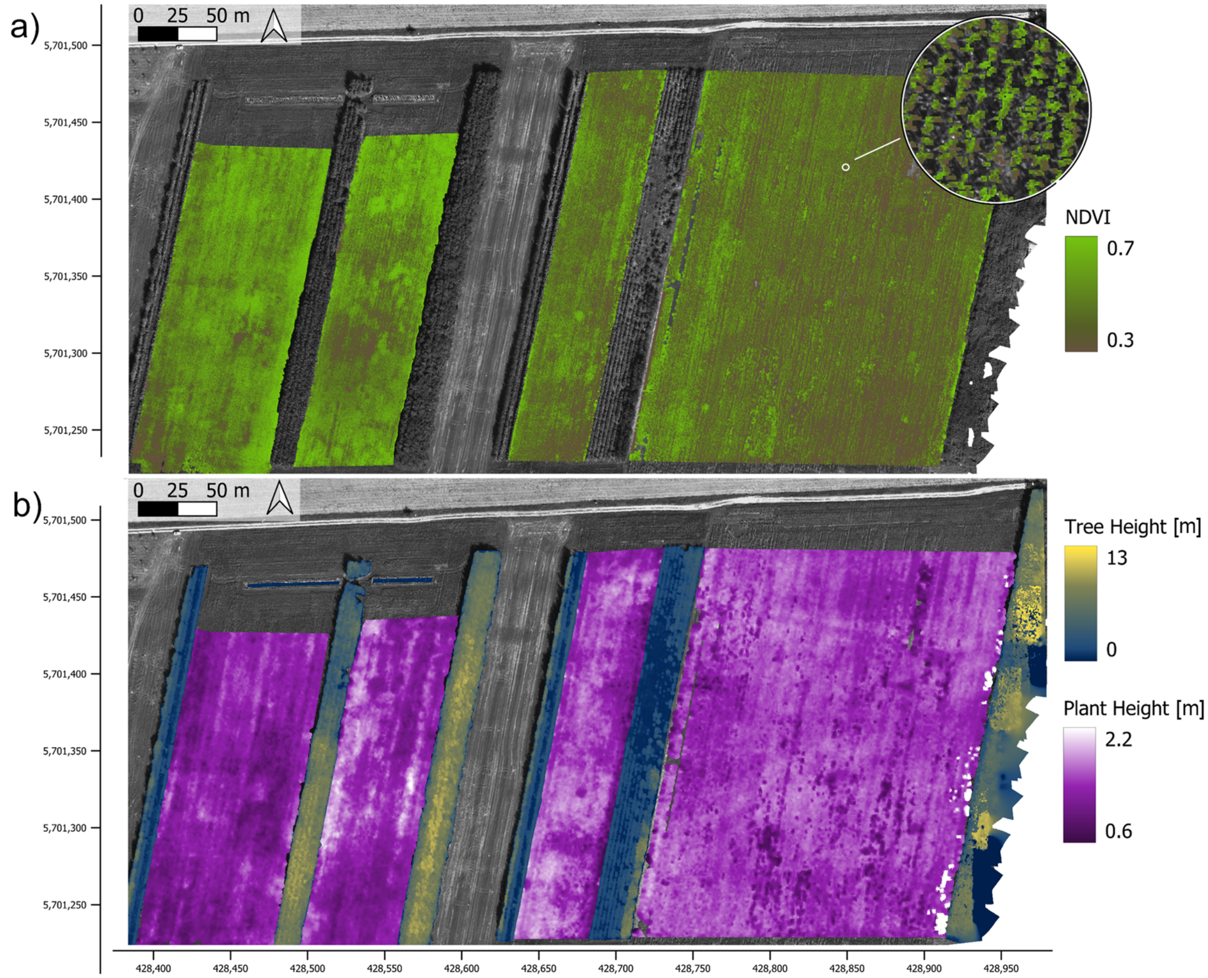

Fig. 2 Spatial distribution of the growth parameters NDVI (upper) and crop and tree height (lower). For the illustration, the values of the mask (NDVI), or the individual height pixels (plant height) were spatially interpolated. It should be noted that this process does not represent soil or weed parameters, but rather provides a spatially comprehensive representation of the plant's NDVI and height. In the NDVI plot, a close-up image is shown in which the masking of the maize plants is visible

and their corresponding height information was extracted from the digital surface model (DSM). A linear plane was fitted using a subset of these points ($n = 10$) to describe the slope of the terrain. The residuals between this plane and the DSM at the remaining ground points were then spatially interpolated using Ordinary Kriging (Krige 1951), resulting in a normalized digital terrain model (nDTM). The nDSM was subsequently obtained by subtracting the nDTM from the DSM.

To determine plant heights and positions, local maxima within the nDSM were identified using a 9×9 pixel moving window, considering only pixels previously classified as maize. To validate the derived heights, a correlation was performed between the nDSM-derived values and reference measurements of 106 plants taken in situ. Because of inherent GPS inaccuracies (see section: UAS Data Acquisition and Processing), the reference heights were compared to the mean nDSM peaks within a 3 m radius. The resulting correlation ($r = 0.84$, Pearson) indicated satisfactory model quality. Finally, a linear model was applied to predict the reference heights, adjusting the gain and offset, which allowed determination of the heights of approximately 85,000 plants.

NDVI adjustment through terrain

The analysis revealed a significant influence of terrain on NDVI variations, with higher NDVI values observed in depressions (Pearson correlations of NDVI to nDTM: Alley 1: −0.32; Alley 2: −0.51; Alley 3: −0.28; Alley 4: −0.02). As this terrain effect could interfere with tree-stripe-derived patterns, a correction method was applied using alley-specific correction factors. In the absence of a reference indicating the exact extent of terrain influence on NDVI, a simplified approach based on correlations and the NDVI distribution was employed:

$$NDVI_{corrected} = NDVI - \left(1 - \frac{H - H_{min}}{H_{max} - H_{min}}\right) * \left(NDVI_{up} - NDVI_{low}\right) * |cor|$$

$NDVI_{corrected}$: NDVI of terrain-corrected pixel.NDVI: NDVI of pixel to be corrected.H: height of pixel to be corrected.$H_{min/max}$: minimum/ maximum height of the terrain in the respective alley.$NDVI_{low / up}$: lower and upper NDVI limits.|cor|: absolute correlation of DTM and NDVI in the respective alley.

The first term in parentheses quantifies the contribution of terrain height: in the lowest depressions, the factor approaches 1, yielding the maximum correction, whereas in terrain peaks, it approaches 0. The NDVI range ($NDVI_{up}$—$NDVI_{low}$) is multiplied by the correlation |cor| to scale the correction appropriately. The NDVI limits were set to 1.5 times the interquartile range (IQR) of the alley-specific NDVI distribution, which effectively excludes outliers. No correction was applied to the plant height model, as no significant correlation with the nDTM was detected.

Regression analyses

To examine the potential influence of the tree stripes, NDVI and plant height were analyzed as functions of distance to the tree stripes. A total of 3000 randomly selected plants were sampled per alley, except for the larger eastern alley, where 15,000 plants were sampled. Although Golicz et al. (2023) recommend multi-level statistical models to account for spatial autocorrelation in agroforestry systems, the uniform random sampling employed here minimizes potential distortion from autocorrelation. Plant heights and NDVI values were extracted within a 1 m radius around each plant. Outliers (1.5 × IQR) were removed in 10 m distance intervals, after which the parameters were plotted against distance to the nearest tree stripe. Splines were fitted to approximate the progression of the parameters, minimizing curvature for visual representation.

The results suggested a distinction between close-range and long-range effects. To analyze these effects in greater detail, the alleys were subdivided into 87 cells, each 25 m wide (Fig. 1, Tree Cells). For each cell, NDVI was plotted against distance, and splines were derived as described above. The effect range was determined as the distance to the first local NDVI minimum observed in the splines, representing the extent of the pronounced close-range NDVI increase typically observed in proximity towards tree stripes. Effect strength was quantified using the R^2 value from linear regression models. For close-range effects, linear regression was applied from 0 m to the effect range, while for long-range effects, regression extended from the effect range to the end of the progression. Additionally, potential relationships between effect range and tree height were investigated by correlating the effect range with nDSM-derived mean tree height within each Tree Cell (Fig. 5).

To further explore long-range effects, direction-dependent regression analyses were conducted to determine whether fluctuations in growth parameters were attributable to tree stripes. If variations were caused by the trees, the explained variance (R^2) or *p*-value would be maximized in the tree direction. To account for any kind of fluctuations in growth parameters, polynomials of degree 10 were tested, of which only significant terms were used for the model. Separate regressions were calculated for each cardinal direction at 1° resolution, using only points located more than 20 m from the nearest tree stripe. Within an alley, regressions were performed separately for the western and eastern sides (Fig. 1), and the results were subsequently merged in the regression plots (Fig. 7).

Results

Spatial representation of maize vitality and maize height

The following results demonstrate a workflow for deriving spatially explicit indicators of maize vitality and height from UAS imagery. Patterns are presented as site-specific outputs rather than generalized effects. Figure 2 illustrates the spatial distribution of NDVI and plant and tree heights. NDVI is higher in the western alleys and lower in the eastern ones. Alley 1 and 2 display a patchy arrangement, with NDVI ranging from 0.3 to 0.7. Plant height patterns are similarly patchy but more evenly distributed across alleys, with Alley 2 showing the highest heights on its western side. No clear correlation exists between plant height and NDVI, and the height model is affected by artefacts at the eastern edge of Alley 4.

Distance to tree stripes relationships of maize growth parameters

The objective was to assess whether spatial patterns in plant growth depend on tree distance. Figure 3 shows that NDVI consistently increases towards tree stripes, with a minimum between 5 and 20 m depending on alley and direction. This close-range increase corresponds to high explanatory variances (R^2) for linear models fitted from 0 m to the first NDVI minimum (Fig. 4). Beyond this minimum, NDVI continues to fluctuate but with low R^2, and no consistent

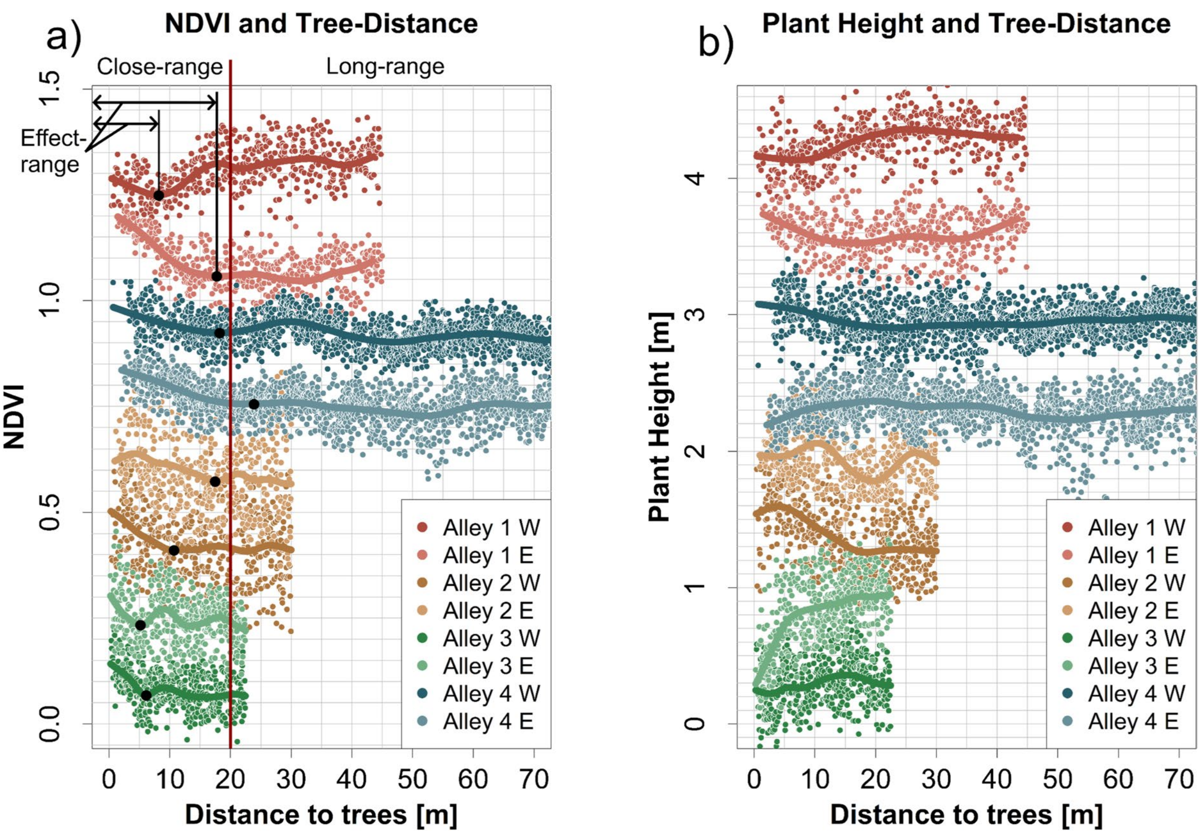

Fig. 3 Growth parameters NDVI and plant height as a function of distance to the nearest tree-stripe, separated by alley and direction (Fig. 1). Sample points and fitted splines illustrate progression. For convenient visualization avoiding overlapping, the progressions are shifted in y-axis (NDVI: A1W: + 0.85, A1E: + 0.6, A2W: + 0.05, A2E: + 0.2, A3W: − 0.27, A3E: − 0.1, A4W: + 0.45, A4E: + 0.33; Plant height: A1W: + 3, A1E: + 2.3, A2W: − 0.1, A2E: + 0.6, A3W: − 1.3, A3E: − 0.6, A4W: + 1.4, A4E: + 0.8). This implies that relative trends are visualized in this figure instead of absolute parameter values

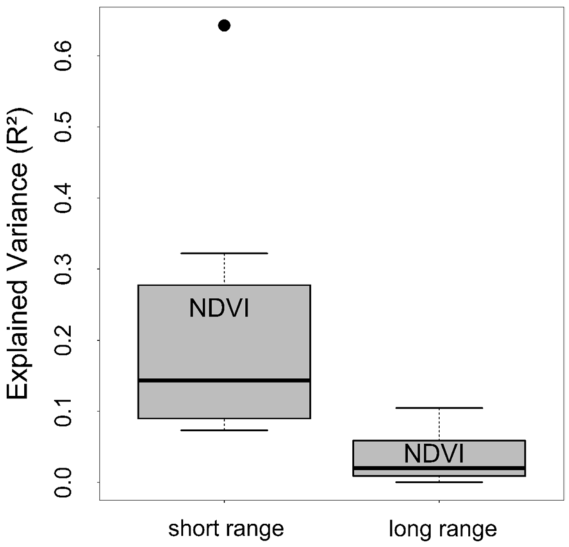

Fig. 4 Explained Variance in NDVI of 87 Linear Models split by Short- and Long Range. The figure illustrates differences in trend strength observed in NDVI obtained from close-range and long-range distances. The variances are illustrated as boxplots for the close-range and long-range linear models. For the close-range models, those that fit the distance from the start of the tree stripe (0 m) to the effect-range were created. The long-range models are fitted from the effect-range to the end of the respective progression. For detailed creation see section Regression Analyses. As the models employed are linear, the boxplots provide an impression of the strength of the trends without considering fluctuations within the progressions

trends are apparent. The pronounced NDVI increase up to 20 m, termed the effect-range, is examined in more detail below. In Alley 4 W and E, NDVI fluctuations appear wave-like, whereas in Alleys 1–3, patterns are inconsistent.

Plant height shows fluctuations of similar magnitude to NDVI, but no consistent trends emerge. Towards tree stripes, increases are observed in Alley 1 W and E and Alley 4 W, while Alley 3 W and E and Alley 4 E display opposite trends. Correlation between NDVI and plant height is variable, ranging from r = 0.48 (Alley 1) to r = −0.26 (Alley 3), with some alleys showing negligible correlation (e.g., Alley 4: r = 0.12).

Correlation analysis indicates a moderate relationship (r = 0.65) between mean tree height and NDVI effect-range: taller trees exert a stronger influence on NDVI (Fig. 5). Effect-range varies from 0 to 25 m, with greater variation for trees taller than 3.5 m. Lower tree heights occur predominantly in Alleys 1 and 3. In this range, some samples exhibited an effect-range of 0 m (see figure description). The fitted linear model ($R^2 = 0.43$, Fig. 5) was employed to schematically illustrate the effect-range of the increasing NDVI (Fig. 6).

Estimation of *effect-range* from tree height

Figure 6 depicts the spatial extent of tree stripe influence on maize NDVI. The schematic illustrates tree stripes 2 and 5 (Fig. 1) along with their corresponding effect-ranges, derived from the linear model shown in Fig. 5. In stripe 2, where tree height predominantly varies along the N-S axis, the NDVI increase extends up to 17 m. In stripe 5, with variation along the W-E axis, the effect-range reaches up to 10 m in the east but scarcely exceeds 5 m in the west. The affected areas cover approximately 1000–3000 m^2 within the 250 m long alleys.

Cardinal regressions

The cardinal regressions for the long-range analysis illustrated in Fig. 7 demonstrate similar patterns of NDVI and plant height within an alley. Alley 1 exhibits a markedly delineated peak, oriented perpendicular to the tree-effect direction and parallel to the length of the alley. The correlation extends up to $R^2 = 0.5$ in the NDVI and $R^2 = 0.22$ in plant height. A more detailed examination of the data indicates a linear trend, with higher values of NDVI and plant heights observed in the northern regions and lower values in the southern regions (data not shown). Other directions show R^2 below 0.1, with minimal evidence of tree-effect direction. A weak peak in NDVI is observed on the eastern side ($R^2 = 0.05$) but is obscured by the north–south trend.

The NDVI in Alley 4 indicates that the explained variance is broadly aligned with the tree direction, with relatively low values of $R^2 = 0.08$ in the west and $R^2 = 0.17$ in the east. Therefore, the *wave-like* patterns observed in Fig. 3 are most pronounced in the direction of the trees. This pattern is not reflected in Alley 4 plant height, as the peaks are pronounced in a north-easterly or south-easterly direction with very low explained variances ($R^2 = 0.05$—0.08).

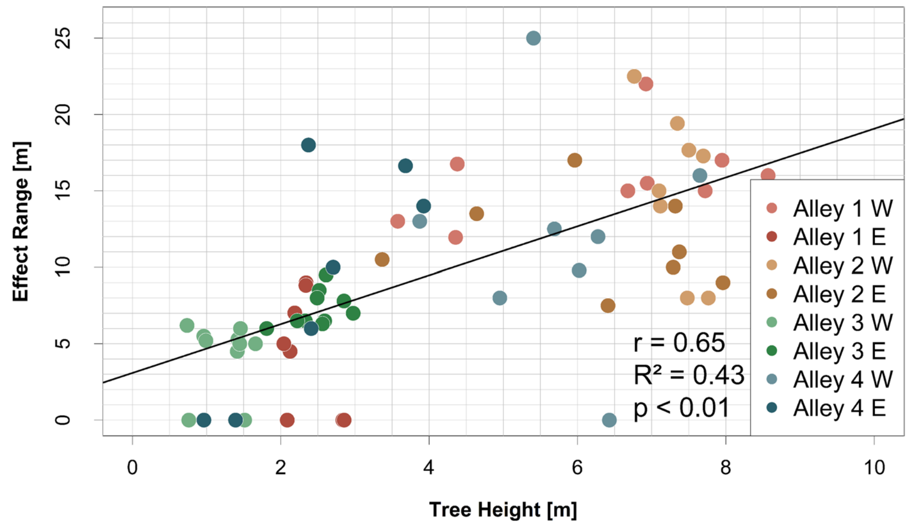

Fig. 5 Pearson correlation analysis of NDVI effect-range and tree height. The analysis, including a linear model, was used to examine the relationship between the close-range NDVI effect range—defined as the distance at which NDVI shows a pronounced increase towards trees (Fig. 3)—and tree height. Calculations were performed separately within 25 m long tree cells (Fig. 1), yielding 78 samples, and correlated with the corresponding mean tree height. Cells in which NDVI increased with distance from the trees were assigned an effect-range of 0 m

Discussion

The patterns observed in this study are discussed as site-specific examples that illustrate the potential of UAS-derived crop metrics in agroforestry systems. They are not intended as broadly generalizable results, but rather to demonstrate the applicability of the methodological approach. With this framing in mind, the discussion begins with an evaluation of growth parameters and maize yield.

Growth parameters and maize yield

To obtain a UAS-based proxy for maize yield, we used NDVI (vitality) together with plant height. Prior work shows that yield predictions improve when plant height complements NDVI rather than using NDVI alone (Yin and McClure 2013; Freeman & Kyle, 2007). In our case, however, plant height and NDVI were only negligibly correlated (Fig. 2), making it difficult to infer yield directly from both. Because plant height showed no consistent spatial pattern—likely reflecting methodological uncertainty—while NDVI did, we interpret results primarily via NDVI and revisit potential height-model issues below (see "Suitability of UAS for Analyzing Agroforestry").

NDVI is widely used to estimate maize yield, either as an additional predictor (Marques Ramos et al. 2020; Yang et al. 2022) or as a standalone indicator (Maresma et al. 2020). Still, the NDVI–yield relationship depends on timing (season, time of day) and other factors (Maresma et al. 2020). Near windbreaks, Iwasaki et al. (2019) even observed a shift from positive (June) to negative (September) correlations. Most studies report positive correlations, especially in later growth stages (Martin et al. 2007; Sunoj et al. 2021). Yang et al. (2022) suggest that the correlation is strongest during the R3 and R4 stages, which correspond to the maize reproductive phases when kernels are in the milk (R3) and dough (R4) stages (Ritchie et al. 1993). These findings align with this study's observations from early September. The correlation can also be influenced by nitrogen application (Maresma et al. 2020). Overall, the NDVI–yield link is strongly context-dependent.

Close-range effects

Within ~ 20 m of tree stripes, both NDVI and plant height varied (Fig. 2), and distance-based plots revealed slight but significant trends (Fig. 3). Close to trees, plant height showed no consistent direction

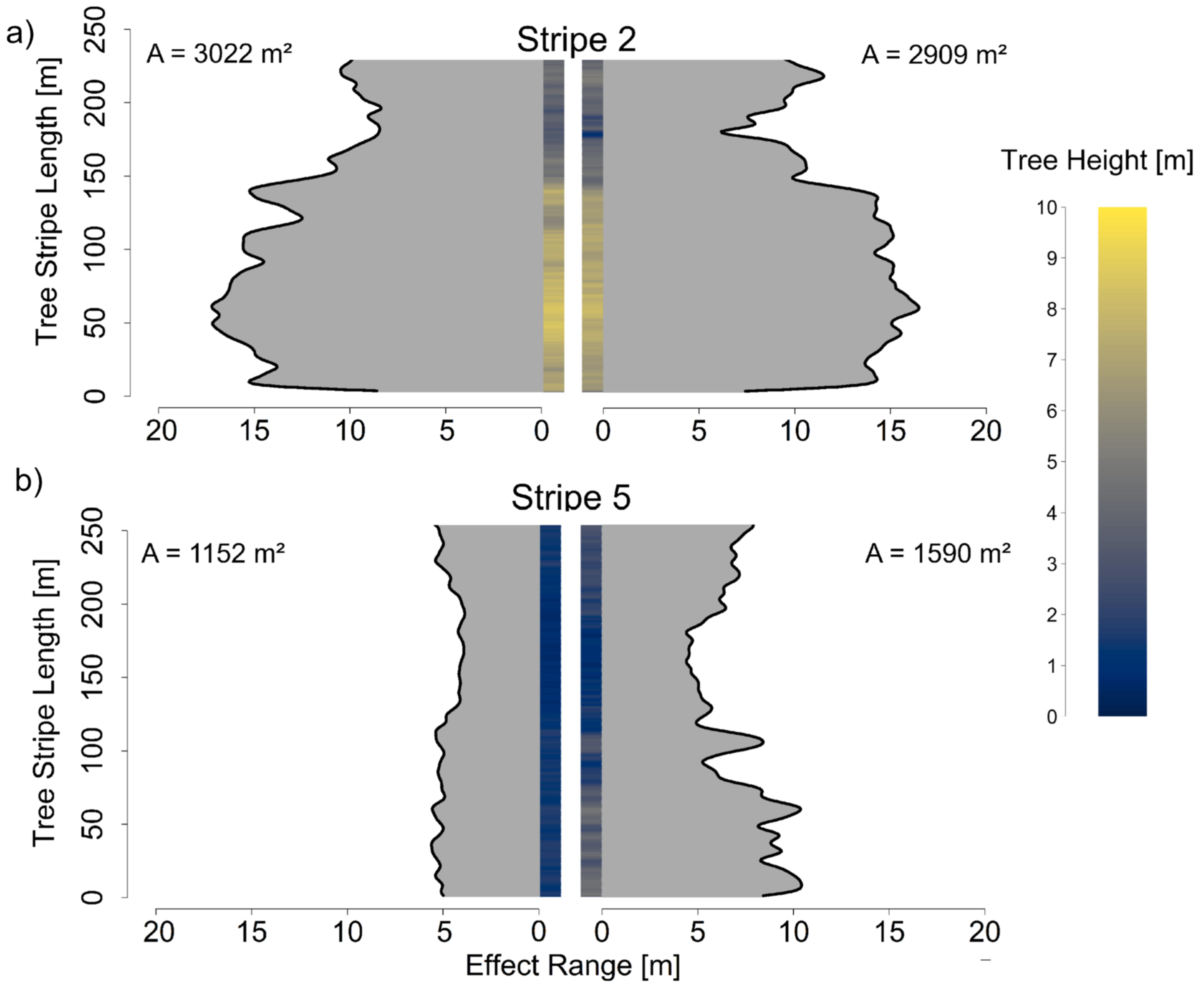

Fig. 6 Schematic representation of two tree stripes and corresponding NDVI effect-range. A (grey area) represents the affected area surrounding the 250 m long tree-stripes

(some alleys increased, others decreased). By contrast, NDVI consistently increased toward trees, typically reaching a minimum within ~ 5–20 m, with alley- and stripe-specific differences (Fig. 3). This pattern occurred across all stripes and scaled with tree height (Fig. 5), indicating a tree-related effect.

The study revealed a spatial pattern showing how tree planting influenced crop growth in the examined AFS. Using NDVI as a proxy for maize yields produced surprising results that contradict the frequently cited competition zone, in which yields typically decline near tree stripes (Majaura, Böhm and Freese, 2024). When interpreting the pattern in terms of windbreak effects, it becomes evident that the spatial extent observed here was considerably smaller than in other reported systems—where positive impacts range from 3–10H (H = tree height) (Cleugh 1998) or 3–5H (Iwasaki et al. 2019). In this study, NDVI increases were restricted to about 0–2.5H, yet a contribution from windbreak effects cannot be excluded. Shading is unlikely to explain the effect, as it typically reduces yields (Majaura, Böhm and Freese, 2024). Instead, improved water availability may have played a role, particularly during dry summer periods, by alleviating water stress and thereby amplifying NDVI signals (Quinkenstein et al. 2009; Bayala and Prieto 2020; Zhang and Zhou 2019). Such improvements could result from reduced evapotranspiration resulting from microclimatic effects (Quinkenstein et al. 2009) or from trees accessing deeper soil layers

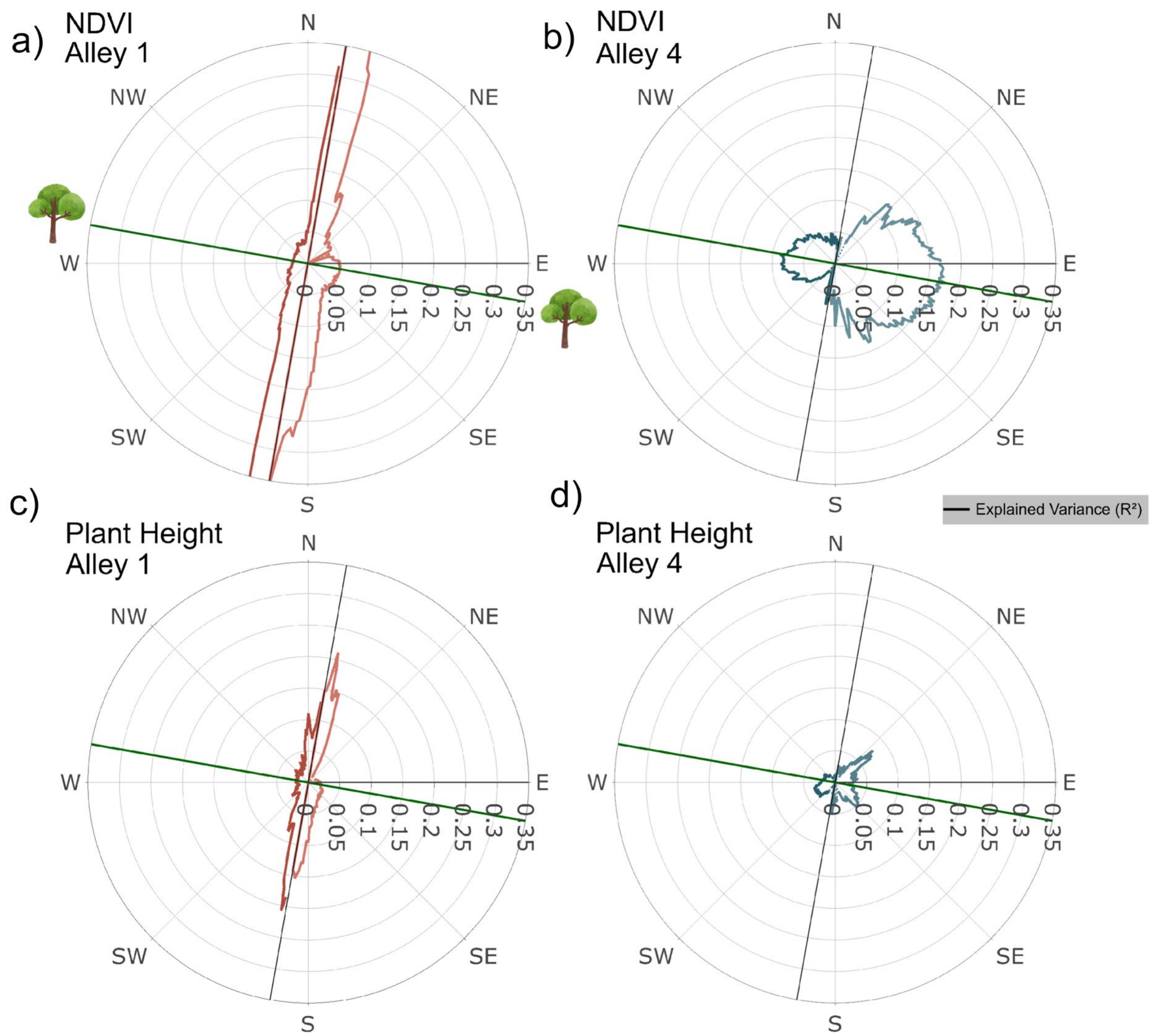

Fig. 7 Variance of growth parameters along cardinal directions. Green line indicates tree stripe direction; black line represents the separation between western and eastern alley sides (Fig. 1). For details of the calculation, see Section Regression Analyses

and redistributing water via hydraulic lift (Bayala and Prieto 2020). However, alternative evidence suggests a more complex picture: Iwasaki et al. (2019) linked NDVI increases near trees to elevated soil temperatures, while reporting reduced soil water content in proximity to tree stripes. Similarly, Pardon et al. (2018) found indications of reduced soil moisture close to trees due to water competition in maize systems, although such a competition zone was not observed in this study.

Another possible factor is an increase in soil organic carbon (SOC), promoted by litterfall, root turnover, and rhizodeposition. SOC stocks are known to increase significantly in temperate AFS (Mayer et al. 2022), which may enhance microbial diversity (Beule, Vaupel and Moran-Rodas, 2022) and, in turn, improve soil fertility. To clarify the mechanisms underlying the observed NDVI increase, future UAS-based studies should be accompanied by in-situ measurements and detailed soil analyses.

Long-range effects

At greater distances, effects were weaker (lower R^2; Fig. 4). NDVI and height still varied, but without consistent monotonic trends (Fig. 3), suggesting no uniform influence on NDVI, height, or yield at long range. Iwasaki et al. (2019) observed NDVI increases out to ~ 3–5H, attributed to wind-related warming; here, consistent effects extended only ~ 0–2.5H.

Figure 7 shows that in Alley 4, plant-height variation peaks toward the southeast and northeast, implying that the height fluctuations in Fig. 3 are largely field-scale heterogeneity rather than tree effects. NDVI variation in Alley 4, however, aligns with tree orientation, indicating tree-related variability. The wave-like NDVI patterns (Fig. 3) could reflect lee-side turbulence (McNaughton 1988; Cleugh 1998), but similar signatures could also arise from mechanical tillage parallel to tree stripes. The form of long-range fluctuations differs among alleys, possibly due to airflow interactions with stripe height/arrangement or to soil heterogeneity (e.g., patchy organic-carbon accumulations from Pleistocene floodplains). Both turbulence and soil variability likely contribute.

Microclimatic effects acting across the whole field could also elevate NDVI broadly, which would be hard to isolate with UAS alone; comparable imagery from nearby non-AFS fields would help. In Alley 4, the higher R^2 values for NDVI and height in the east compared to the west likely reflect the presence of taller trees in that section (Fig. 2). This suggests detectable effects extending toward the mid-alley, but these patterns were not consistent enough to be linked to yield, as no systematic center-directed increases or decreases were observed. The commonly described bell-shaped yield pattern was not confirmed; instead, the opposite tendency (higher yields toward edges, by NDVI proxy) appeared.

Prediction of *effect-range*

Figure 5 shows a moderate but significant correlation between tree height and NDVI effect-range, supporting a height dependency while implying additional drivers. Besides height, species identity and mixtures (Majaura, Böhm and Freese, 2024), geno-/phenotypic variation, and residual soil heterogeneity (despite topographic correction) likely influence effect-range. These were not cosindered in this study due to lack of data.

Compared with our results, Iwasaki et al. (2019) found positive NDVI effects out to 3–5H in a similar maize AFS; differences may reflect wind regime or the relative importance of microclimatic benefits. Roupsard et al. (2020) reported significant NDVI effects within ~ 17 m around trees in a semi-arid West African AFS with pearl millet—broadly consistent in extent with our case—but cross-study comparisons should be cautious given system and climate differences.

To visualize the distance over which trees influence plant growth, Fig. 6 schematically maps the NDVI effect-range for two stripes. While mechanisms remain unresolved, this view helps gauge the spatial extent of tree effects and can inform on-farm economic assessments. Translating NDVI increases into yield gains, however, requires explicit modeling of the NDVI–yield relationship, including management factors such as nitrogen timing.

Suitability of UAS for analyzing agroforestry

This study demonstrates that UAS can resolve spatial fluctuations in AFS. Although effect sizes are modest, large sample sizes ($n \approx 85{,}000$) provide high statistical power. The close-range NDVI increase and its correlation with tree height are readily detected, whereas conventional transects would be laborious (Kanzler et al. 2019; Swieter et al. 2019). UAS workflows also scale: once established, they can be rapidly applied to additional sites (Pádua 2021), enabling efficient, field-scale monitoring.

Limitations remain. DSM-based height retrieval may lack precision for subtle differences, especially given complex maize plant architecture at 60 m flight altitude, which likely contributed to weak height patterns and low NDVI–height correlation. Multiple processing steps can propagate uncertainty, and GPS errors (3–10 m) in manual height sampling complicate validation. Even so, prior work shows UAS DSMs can yield usable crop heights (Gilliot et al., 2021; Oehme et al. 2022). LiDAR could improve structural accuracy but increases study design complexity (Zhang and Grift 2012). On the classification side, edge pixels were often misassigned (maize vs. weeds), biasing toward plant centers; with a 3.1 cm GSD, many pixels are mixed maize–weed/soil.

Without robust classification and validation, reliability is reduced. The absence of a control (non-tree) plot further complicates attribution. Given the multiple overlapping drivers in AFS (Majaura, Böhm and Freese, 2024), analyzing many fields with a consistent workflow is essential.

Yield estimation remains constrained by reliance on spectral indices. NDVI can correlate strongly with yield under good design (Maresma et al. 2020). The EVI (Enhanced Vegetation Index) as an alternative—often used where NDVI saturates (Gitelson et al. 2003)—showed larger within-plant fluctuations in our study which was treated as noise. Direct yield modeling is possible but requires costly ground truth; future models built on large datasets may ease this. With multi-temporal acquisitions and clear knowledge of when parameters correlate best with yield, UAS can robustly delineate AFS patterns. Due to the aforementioned factors, generalization to all agroforestry systems remains challenging; nonetheless, our results provide concrete evidence of tree influences on adjacent crops and demonstrate the field-scale utility of UAS-based analysis.

Conclusions

This study demonstrates that maize plants can be effectively segmented using UAS data and that NDVI reliably reflects yield patterns within AFS. Alongside known ecological benefits, this efficient analytical approach supports broader acceptance of UAS in agricultural practice. Localized NDVI increases were observed near tree stripes, with the strongest effects at 5–20 m into alleys, likely driven by microclimatic reductions in evapotranspiration. Long-range fluctuations may reflect windbreak influences, but no consistent trends were identified. Bell-shaped yield responses were not found; instead, yields increased toward field edges.

Tree effects in this system were present but marginal, with yield gains confined to small spatial scales. The study provides insights into local tree impacts and demonstrates that UAS-based remote sensing can disentangle tree–crop interactions at the field scale, offering a methodological foundation for broader applications. Due to the specificity of this case study, generalization to other agroforestry systems remains limited. Its main contribution lies in showing how high-resolution, spatially explicit UAS data can inform both local analyses and future comparative research in agroforestry.

Acknowledgements We would like to thank the GFZ Helmholtz Centre for Geosciences for providing the equipment for field data collection. Furthermore, we would like to express our gratitude to Domin's Farm Shop for their cooperation in the study and for providing access to the agroforestry system for investigation.

Author's contribution Timo Kunzmann conceptualization (equal), field work (equal), data curation (lead), formal analysis (lead), investigation (lead), methodology (lead), visualization (lead), writing—original draft (lead), writing—review and editing (equal). Carsten Neumann conceptualization (lead), field work (equal), data curation (equal), formal analysis (equal), investigation (equal), methodology (equal), visualization (supporting), writing—original draft (supporting), writing—review and editing (equal). Nicole Koellner conceptualization (equal), field work (equal), data curation (equal), formal analysis (equal), investigation (equal), methodology (supporting), visualization (supporting), writing—original draft (supporting), writing—review and editing (equal).

Funding The research is part of the project "WIR!—LIL—LauMon: Monitoring of cultural landscapes and biodiversity using drones and satellite imagery in the Lausitz region, TP3: multispectral and multitemporal derivation of landscape indicators for the monitoring of transformation processes". It is funded by the Federal Ministry of Education and Research, Germany (BMBF) (grant number: 03WIR3020C). The BMBF supports this project as part of the WIR!—"Wandel durch Innovation in der Region" initiative that is realized in the LIL—"Land-Innovation-Lausitz" alliance. The project supervision and management are implemented by the agency PtJ (Projektträger Jülich).

Data availability The datasets generated during and analyzed during the current study are available from the corresponding author on reasonable request.

Declarations

Conflict of interest The authors declare no conflict of interest.

References

Agisoft LLC. (2023). Agisoft Metashape (Version 2.0) [Photogrammetry software]. https://www.agisoft.com

Awazi, N. P., Njamnjubo, N. A., & Ambebe, T. F. (2024). Agroforestry for ecosystem services: assessing the role of agroforestry for water regulation. Forestist

Bailey NJ, Motavalli PP, Udawatta RP, Nelson KA (2009) Soil CO2 emissions in agricultural watersheds with agroforestry and grass contour buffer strips. Agrofor Syst 77(2):143–158

Bayala J, Prieto I (2020) Water acquisition, sharing and redistribution by roots: applications to agroforestry systems. Plant Soil 453(1):17–28

Beuschel R, Piepho HP, Joergensen RG, Wachendorf C (2019) Similar spatial patterns of soil quality indicators in three poplar-based silvo-arable alley cropping systems in Germany. Biol Fertil Soils 55(1):1–4

Bolívar-Santamaría S, Reu B (2024) Assessing canopy structure in Andean (agro) forests using 3D UAV remote sensing. Agrofor Syst 98(5):1225–1241

Brandle, J. R., Takle, E., & Zhou, X. (2021). Windbreak practices. North Am agrofor, 89–126

Böhm C, Kanzler M, Freese D (2014) Wind speed reductions as influenced by woody hedgerows grown for biomass in short rotation alley cropping systems in Germany. Agrofor Syst 88(4):579–591

Cleugh HA (1998) Effects of windbreaks on airflow, microclimates and crop yields. Agrofor Syst 41(1):55–84

Davis NN, Badger J, Hahmann AN, Hansen BO, Mortensen NG, Kelly M, Larsén XG, Olsen BT, Floors R, Lizcano G, Casso P, Lacave O, Bosch A, Bauwens I (2023) Oliver James Knight, Albertine Potter van Loon, Rachel Fox, Tigran Parvanyan, Søren Bo Krohn Hansen, Duncan Heathfield, Marko Onninen, Ray Drummond; The Global Wind Atlas: A high-resolution dataset of climatologies and associated web-based application. Bull Am Meteor Soc 104(8):E1507–E1525

Davis KF, Gephart JA, Emery KA, Leach AM, Galloway JN, D'Odorico P (2016) Meeting future food demand with current agricultural resources. Glob Environ Change 1(39):125–132

Wetterdienst D (2023) Bericht zur Witterung im Sommer 2023. Retrieved July 3, 2024 from https://www.dwd.de/DE/fachnutzer/landwirtschaft/berichte/pdfs/2023_bericht_sommer_berrierefrei.pdf?__blob=publicationFile&v=2

Dmuchowski W, Baczewska-Dąbrowska AH, Gworek B (2024) The role of temperate agroforestry in mitigating climate change: A review. For Policy Econ 1(159):103136

Drastig, K. et al. (2011) Agricultural water management in Brandenburg, DIE ERDE—Journal of the Geographical Society of Berlin, 142(1–2), 119–140

EU CAP network. analytical work—supporting the establishment of agroforestry systems; EU CAP network: Brussels, Belgium, 2023

Freeman KW, Girma K, Arnall DB, Mullen RW, Martin KL, Teal RK, Raun WR (2007) By-plant prediction of corn forage biomass and nitrogen uptake at various growth stages using remote sensing and plant height. Agro J 99(2):530–536

Gago J, Douthe C, Coopman RE, Gallego PP, Ribas-Carbo M, Flexas J, Escalona J, Medrano H (2015) UAVs challenge to assess water stress for sustainable agriculture. Agric Water Manag 1(153):9–19

Geoportal LBGR Brandenburg. (2024). Retrieved July 3, 2024, from https://geo.brandenburg.de/

Ghale, B., Mitra, E., Sodhi, H. S., Verma, A. K., & Kumar, S. (2022). Carbon sequestration potential of agroforestry systems and its potential in climate change mitigation. Water, Air, & Soil Pollution, 233(7), 228.Gilliot, J.M. et al. (2021) An accurate method for predicting spatial variability of maize yield from UAV-based plant height estimation: a tool for monitoring agronomic field experiments, Precis Agric 22(3), 897–921.https://doi.org/10.1007/s11119-020-09764-w

Gitelson AA et al (2003) 'Remote estimation of leaf area index and green leaf biomass in maize canopies', geophysical research letters, 30(5). Available. https://doi.org/10.1029/2002GL016450

Golicz K, Piepho HP, Minarsch EM, Niether W, Große-Stoltenberg A, Oldeland J, Breuer L, Gattinger A, Jacobs S (2023) Highlighting the potential of multilevel statistical models for analysis of individual agroforestry systems. Agrofor Syst 97(8):1481–1489

Holman FH, Riche AB, Michalski A, Castle M, Wooster MJ, Hawkesford MJ (2016) High throughput field phenotyping of wheat plant height and growth rate in field plot trials using uav based remote sensing. Remote Sens 8(12):1031

Iwasaki K, Torita H, Abe T, Uraike T, Touze M, Fukuchi M, Sato H, Iijima T, Imaoka K, Igawa H (2019) Spatial pattern of windbreak effects on maize growth evaluated by an unmanned aerial vehicle in Hokkaido, Northern Japan. Agrofor Syst 93(3):1133–1145

Jacobs SR, Webber H, Niether W, Grahmann K, Lüttschwager D, Schwartz C, Breuer L, Bellingrath-Kimura SD (2022) Modification of the microclimate and water balance through the integration of trees into temperate cropping systems. Agric for Meteorol 15(323):109065

Kanzler, M. et al. (2019) Microclimate effects on evaporation and winter wheat (Triticum aestivum L.) yield within a temperate agroforestry system, Agroforestry Systems, 93(5), 1821–1841. Available at: https://doi.org/10.1007/s10457-018-0289-4

Kasperski M (2002) A new wind zone map of Germany. J Wind Eng Ind Aerodyn 90(11):1271–1287

Kaushal, R., Mandal, D., Panwar, P., Kumar, P., Tomar, J. M. S., & Mehta, H. (2021). Soil and water conservation benefits of agroforestry. In Forest resources resilience and conflicts (pp. 259–275). Elsevier

Kim KE (1996) Adaptive majority filtering for contextual classification of remote sensing data. Int J Remote Sens 17(5):1083–1087

Kim DG, Isaac ME (2022) Nitrogen dynamics in agroforestry systems. Rev Agron Sustain Dev 42(4):60

Klose S, Koch J, Bäucker E, Makeschin F (2001) Indicative properties of fly-ash affected forest soils in Northeastern Germany. J Plant Nutr Soil Sci 164(5):561–568
Kokaly RF, Clark RN (1999) Spectroscopic determination of leaf biochemistry using band-depth analysis of absorption features and stepwise multiple linear regression. Remote Sens Environ 67(3):267–287
Kopp, D. and Schwanecke, W. (no date) Standörtlich-naturräumliche Grundlagen ökologiegerechter Forstwirtschaft
Krige DG (1951) A statistical approach to some basic mine valuation problems on the Witwatersrand. J South Afr Inst Min Metall 52(6):119–139
L Breiman 2001 Random Forests Machine Learning 45 5 32
Leroux L, Falconnier GN, Diouf AA, Ndao B, Gbodjo JE, Tall L, Balde AA, Clermont-Dauphin C, Bégué A, Affholder F, Roupsard O (2020) Using remote sensing to assess the effect of trees on millet yield in complex parklands of Central Senegal. Agric Syst 1(184):102918
Li J, Heap AD (2014) Spatial interpolation methods applied in the environmental sciences: A review. Environ Model Softw 1(53):173–189
Majaura M, Böhm C, Freese D (2024) The influence of trees on crop yields in temperate zone alley cropping systems: a review. Sustainability 16(8):3301
Mantel S, Dondeyne S, Deckers S (2023) World reference base for soil resources (WRB). Encycl Soils Environ 1(4):206–217
Maresma A, Chamberlain L, Tagarakis A, Kharel T, Godwin G, Czymmek KJ, Shields E, Ketterings QM (2020) Accuracy of NDVI-derived corn yield predictions is impacted by time of sensing. Comput Elect Agric 1(169):105236
Martin KL, Girma K, Freeman KW, Teal RK, Tubaña B, Arnall DB, Chung B, Walsh O, Solie JB, Stone ML, Raun WR (2007) Expression of variability in corn as influenced by growth stage using optical sensor measurements. Agron J 99(2):384–389
Mayer S, Wiesmeier M, Sakamoto E, Hübner R, Cardinael R, Kühnel A, Kögel-Knabner I (2022) Soil organic carbon sequestration in temperate agroforestry systems–A meta-analysis. Agric Ecosyst Environ 1(323):107689
McNaughton, K.G. (1988) 1. Effects of windbreaks on turbulent transport and microclimate, Agriculture, Ecosystems & Environment, 22–23, pp. 17–39. Available at: https://doi.org/10.1016/0167-8809(88)90006-0
Molotoks A, Smith P, Dawson TP (2021) Impacts of land use, population, and climate change on global food security. Food Energy Secur 10(1):e261
Mosquera-Losada MR, Santos MG, Gonçalves B, Ferreiro-Domínguez N, Castro M, Rigueiro-Rodríguez A, González-Hernández MP, Fernández-Lorenzo JL, Romero-Franco R, Aldrey-Vázquez JA, Sobrino CC (2023) Policy challenges for agroforestry implementation in Europe. Front for Glob Change 14(6):1127601
Mosquera-Losada, M.R. et al. (2012) Past, Present and Future of Agroforestry Systems in Europe, in P.K.R. Nair and D. Garrity (eds) Agroforestry—The future of global land use. Dordrecht: Springer Netherlands, pp. 285–312. Available at: https://doi.org/10.1007/978-94-007-4676-3_16
Nair, P.K.R. (1985) Classification of agroforestry systems, Agroforestry Systems, 3(2), pp. 97–128. Available at: https://doi.org/10.1007/BF00122638
Nevavuori P, Narra N, Lipping T (2019) Crop yield prediction with deep convolutional neural networks. Comput Elect Agric 1(163):104859
Niblack, W. (1985) An introduction to digital image processing. Guide Books
Nuberg IK (1998) Effect of shelter on temperate crops: a review to define research for Australian conditions. Agrofor Syst 41(1):3–34
Oehme LH, Reineke AJ, Weiß TM, Würschum T, He X, Müller J (2022) Remote sensing of maize plant height at different growth stages using UAV-based digital surface models (DSM). Agronomy 12(4):958
Oliver MA, Webster R (1990) Kriging: a method of interpolation for geographical information systems. Int J Geograp Inf Syst 4(3):313–332
Palma, J.H.N. et al. (2007) Methodological approach for the assessment of environmental effects of agroforestry at the landscape scale, Ecological Engineering, 29(4), pp. 450–462. Available at: https://doi.org/10.1016/j.ecoleng.2006.09.016
Pardon P, Reubens B, Mertens J, Verheyen K, De Frenne P, De Smet G, Van Waes C, Reheul D (2018) Effects of temperate agroforestry on yield and quality of different arable intercrops. Agric Syst 1(166):135–151
Pardon P, Reubens B, Reheul D, Mertens J, De Frenne P, Coussement T, Verheyen K (2017) Trees increase soil organic carbon and nutrient availability in temperate agroforestry systems. Agric Ecosyst Environ 247:98–111
Pádua L, Vanko J, Hruška J, Adão T, Sousa JJ, Peres E, Morais R (2017) UAS, sensors, and data processing in agroforestry: a review towards practical applications. Int J Remote Sens 38(8–10):2349–2391
Pádua, L.F.M. (2021) Automatic analysis of UAS-based multi-temporal data as support to a precision agroforestry management system. Available at: http://hdl.handle.net/10348/10417 (Accessed: 26 June 2024)
Quinkenstein A, Wöllecke J, Böhm C, Grünewald H, Freese D, Schneider BU, Hüttl RF (2009) Ecological benefits of the alley cropping agroforestry system in sensitive regions of Europe. Environ Sci Policy 12(8):1112–1121
Ramos AP, Osco LP, Furuya DE, Gonçalves WN, Santana DC, Teodoro LP, da Silva Junior CA, Capristo-Silva GF, Li J, Baio FH, Junior JM (2020) A random forest ranking approach to predict yield in maize with uav-based vegetation spectral indices. Comput Electr Agric 1(178):105791
Ritchie, S.W., J.J. Hanway, G.O. Benson, and J.C. Herman. 1993. How a corn plant develops, Special Report, No. 48, Iowa State University
Roupsard O, Audebert A, Ndour AP, Clermont-Dauphin C, Agbohessou Y, Sanou J, Koala J, Faye E, Sambakhe D, Jourdan C, Le Maire G (2020) How far does the tree affect the crop in agroforestry? New spatial analysis methods in a Faidherbia parkland. Agric Ecosyst Environ 1(296):106928
Rumpel C, Knicker H, Kögel-Knabner I, Hüttl RF (1998) Airborne contamination of immature soil (lusatian mining district) by lignite-derived materials: its detection and contribution to the soil organic matter budget. Water, Air, and Soil Pollut 105(1):481–492

Santiago-Freijanes JJ, Mosquera-Losada MR, Rois-Díaz M, Ferreiro-Domínguez N, Pantera A, Aldrey JA, Rigueiro-Rodríguez A (2021) Global and European policies to foster agricultural sustainability: agroforestry. Agrofor Syst 95(5):775–790

Shi L, Feng W, Xu J, Kuzyakov Y (2018) Agroforestry systems: Meta-analysis of soil carbon stocks, sequestration processes, and future potentials. Land Degrad Dev 29(11):3886–3897

Sileshi GW, Mafongoya PL, Nath AJ (2020) Agroforestry systems for improving nutrient recycling and soil fertility on degraded lands. Agrofor Degrad Lands Recent Adv Emerg Chall-Vol 1:225–253

Sinclair FL (1999) A general classification of agroforestry practice. Agrofor Syst 46(2):161–180

Smith J, Pearce BD, Wolfe MS (2013) Reconciling productivity with protection of the environment: Is temperate agroforestry the answer? Renew Agric Food Syst 28(1):80–92

Sollen-Norrlin M, Ghaley BB, Rintoul NLJ (2020) Agroforestry benefits and challenges for adoption in Europe and beyond. Sustainability 12(17):7001

Sunoj S, Cho J, Guinness J, van Aardt J, Czymmek KJ, Ketterings QM (2021) Corn grain yield prediction and mapping from unmanned aerial system (UAS) multispectral imagery. Remote Sens 13(19):3948

Swieter A, Langhof M, Lamerre J, Greef JM (2019) Long-term yields of oilseed rape and winter wheat in a short rotation alley cropping agroforestry system. Agrofor Syst 93(5):1853–1864

Thapa B, Lovell S, Wilson J (2023) Remote sensing and machine learning applications for aboveground biomass estimation in agroforestry systems: a review. Agrofor Syst 97(6):1097–1111

Thiesmeier A, Zander P (2023) Can agroforestry compete? A scoping review of the economic performance of agroforestry practices in Europe and North America. For Policy Econ 150:102939

Torralba M, Fagerholm N, Burgess PJ, Moreno G, Plieninger T (2016) Do European agroforestry systems enhance biodiversity and ecosystem services? A meta-analysis. Agric Ecosyst Environ 16(230):150–161

Tsonkova P, Böhm C, Quinkenstein A, Freese D (2012) Ecological benefits provided by alley cropping systems for production of woody biomass in the temperate region: a review. Agrofor Syst 85(1):133–152

Tsouros DC, Bibi S, Sarigiannidis PG (2019) A review on UAV-based applications for precision agriculture. Information 10(11):349

Wengert M, Piepho HP, Astor T, Graß R, Wijesingha J, Wachendorf M (2021) Assessing spatial variability of barley whole crop biomass yield and leaf area index in Silvoarable agroforestry systems using UAV-borne remote sensing. Remote Sens 13(14):2751

Weninger T, Scheper S, Lackóová L, Kitzler B, Gartner K, King NW, Michel K (2021) Ecosystem services of tree windbreaks in rural landscapes—a systematic review. Environ Res Lett 16(10):103002

Yang KF et al (2020) Forest edges near farms enhance wheat productivity measures: a test using high spatial resolution remote sensing of smallholder farms in Southern Ethiopia, frontiers in sustainable food systems, 4. Available at: https://doi.org/10.3389/fsufs.2020.00130

Yang B, Zhu W, Rezaei EE, Li J, Sun Z, Zhang J (2022) The optimal phenological phase of maize for yield prediction with high-frequency UAV remote sensing. Remote Sens 14(7):1559

Yin X, McClure MA (2013) Relationship of corn yield, biomass, and leaf nitrogen with normalized difference vegetation index and plant height. Agron J 105(4):1005–1016

Zhang L, Grift TE (2012) A LIDAR-based crop height measurement system for Miscanthus giganteus. Comput Elect Agric 1(85):70–76

Zhang F, Zhou G (2019) Estimation of vegetation water content using hyperspectral vegetation indices: a comparison of crop water indicators in response to water stress treatments for summer maize. BMC Ecol 19(1):18

Zhang, H. et al. (2019) Evaluating the potential of post-processing kinematic (PPK) georeferencing for UAV-based structure- from-motion (SfM) photogrammetry and surface change detection, Earth Surface Dynamics, 7(3), pp. 807–827. Available at: https://doi.org/10.5194/esurf-7-807-2019

Zhu X, Liu W, Chen J, Bruijnzeel LA, Mao Z, Yang X, Cardinael R, Meng FR, Sidle RC, Seitz S, Nair VD (2020) Reductions in water, soil and nutrient losses and pesticide pollution in agroforestry practices: a review of evidence and processes. Plant Soil 453(1):45–86